Synthesis of Pt Nanoparticles and Nanorods by Microwave-assisted Solvothermal Technique

Dongsheng Li and Sridhar Komarneni

Materials Research Institute, Materials Research Laboratory, The Pennsylvania State University, University Park, Pennsylvania 16802, USA

Reprint requests to Prof. Dr. S. Komarneni. E-mail: komarneni@psu.edu

Platinum nanoparticles and nanorods were synthesized by microwave-assisted solvothermal techniques. Changing the reaction conditions controlled particle size and morphology. The effects of the reaction conditions, such as the molar ratio of the polyvinylpyrrolidone (PVP) repeating unit to the metal sources, the concentration of metal sources, the reaction temperature, and the presence of distilled water were investigated. Nanoparticles of Pt were approximately 3 nm in size. Produced nanoparticles and nanorods were characterized by transmission electron microscopy. Image J™ software was used to calculate the particle size and size distribution.

Key words: Nanoparticles, Nanorods, Platinum, Microwave-assisted Techniques

Introduction

Platinum nanoparticles currently are of intense interest due to their unique catalytic properties. A range of organic chemical reactions can be catalyzed by Pt nanoparticles such as hydrosilylation, oxidation, and hydrogenation [1]. Furthermore, Pt nanoparticles are catalytically active in r. t. electro-oxidation reactions for fuel cell applications [2]. Pt nanoparticles have been deposited in multilayer films and used as electrocatalysts for dioxygen reduction [3]. Therefore, the synthesis of Pt nanoparticles has developed into an increasingly important research area. It is well-known that the catalytic activity of the metal is strongly dependent on the particle shape, size, and size distribution [4]. Many methods have been developed for the synthesis of Pt nanoparticles and for controlling the particle size and shape [4 – 15]. Lately, dendrimers have been used as templates to produce Pt nanoparticles and the catalytic properties of the encapsulated Pt nanoparticles have been studied [13, 16, 17]. Pt nanoparticles with well-controlled shape (cubic and tetrahedral shapes) have been synthesized by changing the ratio of the capping polymer material (sodium polyacrylate) to the concentration of the platinum cations [4]. In this work, Pt nanoparticles have been prepared with methanol and ethanol as reducing agents by microwave-assisted solvothermal techniques.

Table 1. List of the concentrations of chemicals, volumes of methanol and ethanol, molar ratio of PVP repeating unit to Pt^{4+}, and the reaction temperature of solutions for 60 min.

Sample code	$c_{\text{Metal precursor}}$, mM H_2PtCl_6	c_{PVP}, mM MW 40 K	R	V_{methanol}, mL	V_{ethanol}, mL	T, °C
1	9	0.4	18		10	90
2	9	0.04	1.8		10	90
3	9	0.04	1.8		10	120
4	9	0.4	18	10		90
5	9	0.04	1.8	10		90
6	9	0.04	1.8	10		120

R: molar ratio of PVP repeating unit to metal precursor.

Experimental Section

Polyvinylpyrrolidone (PVP) with an average molecular weight of 40 K [18] was first dissolved in methanol or ethanol. Methanol and ethanol act as both reducing agent and solvent in the synthesis procedure. Dihydrogen hexachloroplatinate(IV) was used as a metal precursor. This metal source was added to the methanol-PVP and ethanol-PVP solutions. Distilled water was added in the case of methanol to investigate the effect of water on the morphology. Tables 1 and 2 list the quantities of chemicals and volumes of methanol and ethanol used in the synthesis. The reactants were heated at 90 or 120 °C for 60 min by using a microwave-accelerated reaction system. The microwave-assisted experiments were performed using a MARS-5 (CEM corp., Matthews, NC) microwave digestion system. The microwave system operated at a frequency of 2.45 GHz with a maxi-
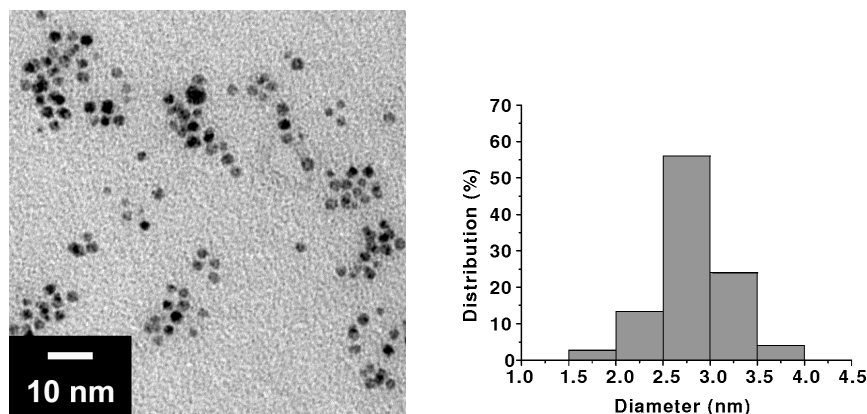
Fig. 1. TEM image (left) and size distribution histogram (right) of Pt nanoparticles (sample 6) formed with PVP (0.04 mM) and Pt^{4+} (9 mM) at 120 °C without distilled water but with methanol as a reducing agent.

Table 2. List of the concentrations of chemicals, volumes of methanol and distilled water, molar ratio of PVP repeating unit to Pt^{4+}, and the reaction temperature of solutions for 60 min.

Sample code	$c_{Metal\ precursor}$, mM H_2PtCl_6	c_{PVP}, mM MW 40 K	R	$V_{methanol}$, mL	V_{water}, mL	T, °C
7	0.9	0.04	18	9	1	90
8	0.9	0.04	18	9	1	120
9	0.9	0.04	18	10	–	90
10	0.9	0.01	4.5	9	1	90
11	0.9	0.06	27	9	1	90
12	0.9	0.16	72	9	1	90
13	0.15	0.04	108	9	1	90
14	0.6	0.04	27	9	1	90
15	0.75	0.04	21	9	1	90
16	1.05	0.04	15	9	1	90
17	2.4	0.04	6.7	9	1	90

Fig. 2. EDS spectrum of Pt nanoparticles shown in Fig. 1 (left).

mum power of 1200 W. The experiments were carried out in double-walled digestion vessels having an inner non-reactive teflon PFA liner and an outer ultem polyetherimide shell of high mechanical strength. Temperature and pressure probes allowed the reaction to be controlled by monitoring the temperature and pressure within a control vessel. The maximum operating temperature and pressure for the system were 240 °C and 350 psi, respectively. The pressure was below 200 psi in these experiments. The particle size, shape, size distribution, and state of aggregation were determined by a Philips 420 or JEOL 2010F transmission electron microscope operated at 120 and 200 KeV, respectively. The TEM samples were prepared by placing several drops of the reaction solution onto a carbon-coated copper grid (300 mesh), followed by evaporating the ethanol in air at r. t.. The particle size distribution was calculated with the Image J^{TM} software by randomly collecting about 100 nanoparticles, and the particle size was calculated based on a 95% confidence interval.
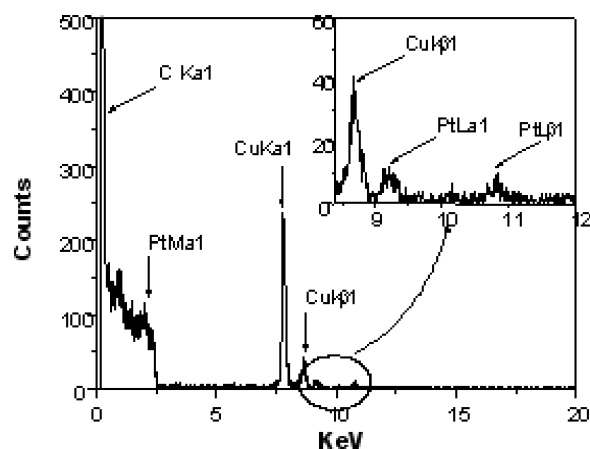
Results and Discussion

Synthesis of Pt nanoparticles without distilled water

When methanol was used as a reducing agent, with concentrations of Pt^{4+} and PVP of 9 mM and 0.04 mM, respectively, well crystallized and monodispersed Pt nanoparticles were obtained after 60 min at 120 °C. Fig. 1 gives the TEM image and particle size distribution histogram of the synthesized Pt nanoparticles. The size distribution histogram shows that Pt nanoparticles are more or less monodispersed and the size of the nanoparticles is approximately 3 nm on the average. Fig. 2 shows the EDS spectrum of the nanoparticles given in Fig. 1 (left). The EDS spectrum proves the formation of Pt metal nanoparticles. High intensity peaks corresponding to Cu and C in the EDS spectrum result from the copper grid with its carbon film. The EDS peaks corresponding to Pt are very small because
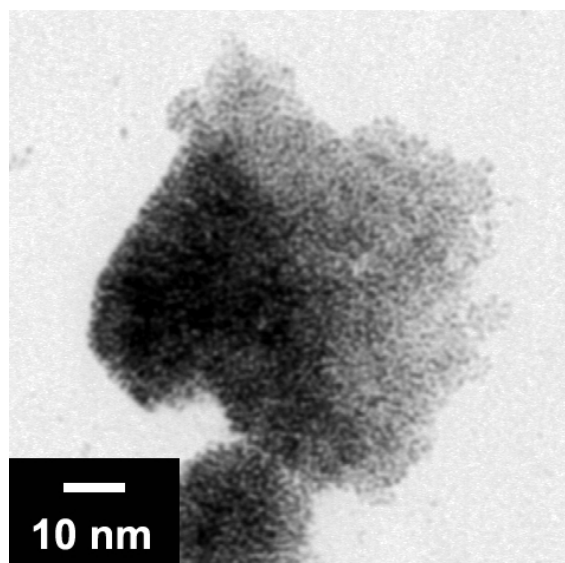
Fig. 3. TEM Image of agglomerated Pt nanoparticles (sample 5) formed with PVP (0.04 mM) and Pt^{4+} (9 mM) at 90 °C for 60 min with methanol as a reducing agent.
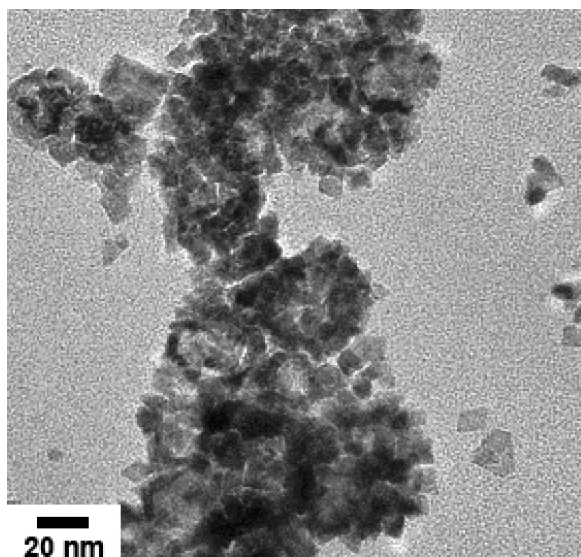

Fig. 4. TEM image of Pt nanoparticles (sample 3) synthesized at 120 °C by using ethanol as a reducing agent.

only a small amount of Pt nanoparticles was collected. The morphology of the Pt particles was affected by the reaction temperature. Agglomerated Pt nanoparticles formed when the sample was heated for 60 min at 90 °C, as shown in Fig. 3. The lower temperature of 90 °C led to smaller nanoparticles as compared to those synthesized at 120 °C. Therefore, the higher sur-

face energy due to smaller particles resulted in the agglomeration of Pt nanoparticles.

When ethanol was used as a reducing agent, Pt nanoparticles did not form at 90 °C after treatment for 1 h. However, at 120 °C agglomerated Pt nanoparticles were obtained (Fig. 4).

Synthesis of Pt nanoparticles with distilled water in methanol

With the presence of distilled water in the reaction system, Pt nanorods were obtained and the effects of concentration of the metal source and the reaction temperature were studied.

Effect of concentration of the Pt^{4t} metal source on the morphology of Pt nanoparticles

With a certain amount of distilled water in the reaction system, Pt nanorods formed. When the reactants were prepared with a low concentration of Pt^{4+} (around 0.90 mM) and a PVP concentration of 0.04 mM, agglomerated Pt nanorods formed at 90 °C within 60 min. The morphology of Pt nanoparticles is dependent on the concentrations of Pt^{4+} and PVP. Fig. 5 presents the TEM images and the major and minor axis size distribution of Pt nanorods synthesized with different concentrations of Pt^{4+}. At a concentration of 0.9 mM, more Pt nanorods were obtained. At lower or higher concentration of 0.75 mM or 2.4 mM, fewer Pt nanorods were produced. Size distributions (Fig. 5) show that the minor axis length of nanospheres is in the range of about 2 to 5 nm and the length of the nanorods is approximately 5 to 10 nm. The particle size of the Pt nanospheres synthesized at a low Pt^{4+} concentration of 0.75 mM ranges from 2 to 4 nm and the length of the major axis of the Pt nanorods varies from about 5 to 8 nm. With even higher Pt^{4+} concentrations of 0.9 mM and 2.4 mM, the particle size of the Pt nanospheres is larger ranging from 3 to 5 nm and the length of the major axis of the Pt nanorods ranges from 6 to 10 nm. The major axis of the nanorods was approximately twice to four times as long as the minor axis. With higher Pt^{4+} concentrations, particle size increases, while only a Pt^{4+} concentration of about 0.9 mM produces more nanorods.

The possible mechanism of the growth of nanorods is that nanospheres formed first. Then two or more nanospheres self-assemble and grow as nanorods. Another possible mechanism is that nanorods grow from
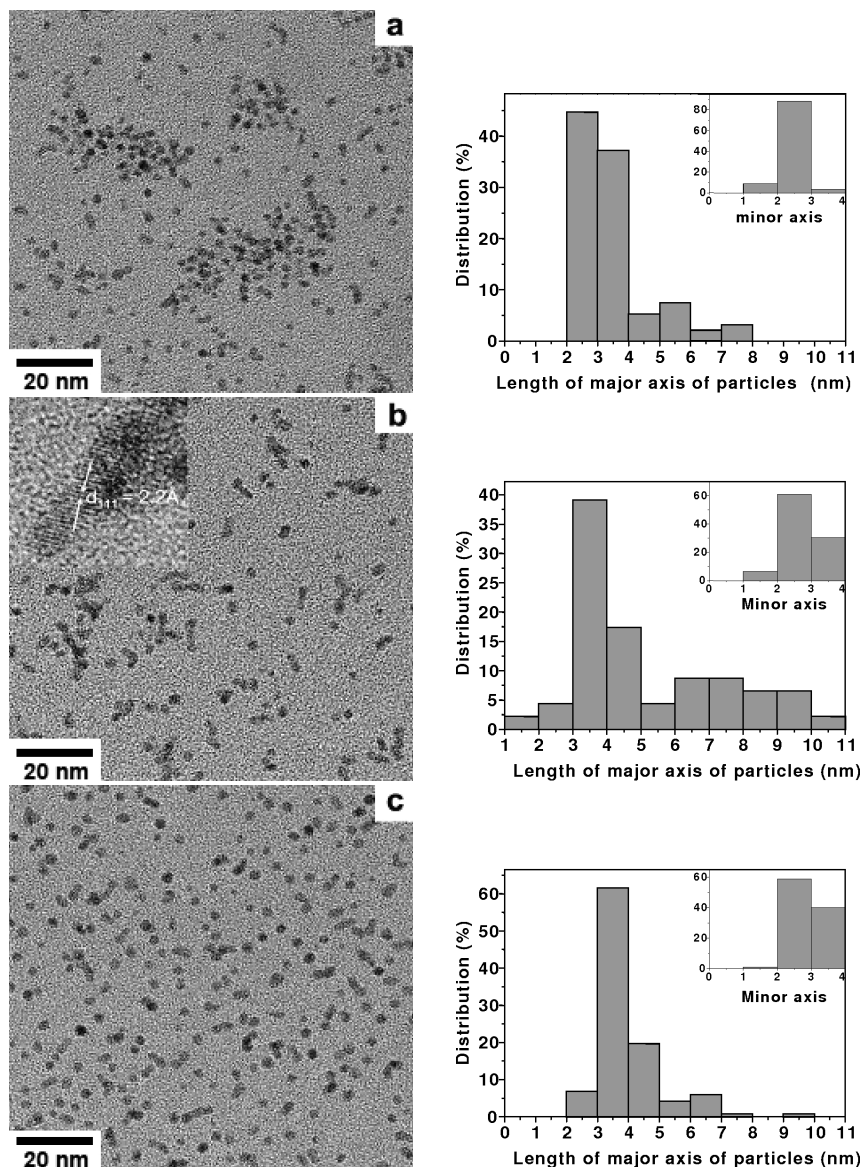
Fig. 5. TEM images and major axis size distribution of Pt nanorods synthesized with PVP concentration of 0.04 mM but with different Pt^{4+} concentrations of, (a) 0.75 mM (sample 15); (b) 0.9 mM (sample 7); and (c) 2.4 mM (sample 17) at 90 °C for 60 min. Inset of Fig. b (TEM image) shows the high resolution TEM image of a single nanorod.

the nanospheres along a certain direction. Both mechanisms assume that the resulting nanospheres were not fully covered by the protecting agent (PVP), with the PVP molecules probably being bonded to certain planes while others were not coordinated, which may have led to the preferential growth of nanorods. The former mechanism seems more likely because it can be seen from the TEM pictures (Fig. 5) that there are some nanospheres, which agglomerated. That the major axes were two or four times longer than the minor axes further suggests the former mechanism. For either of the mechanisms, low Pt^{4+} concentrations led to low concentrations of the formed nanospheres. Therefore, the possibility for the nanospheres to self-assemble is low (for the former mechanism) or there are not enough Pt^{4+} ions for the growth of nanorods (for the latter mechanism). The higher concentration of Pt^{4+} led to a lower PVP to Pt ratio, which gave rise to even less protecting agent (PVP) surrounding the Pt nanospheres. This probably resulted in larger particle sizes instead of nanorods (shown in inset of minor axis size distribution in Fig. 5).
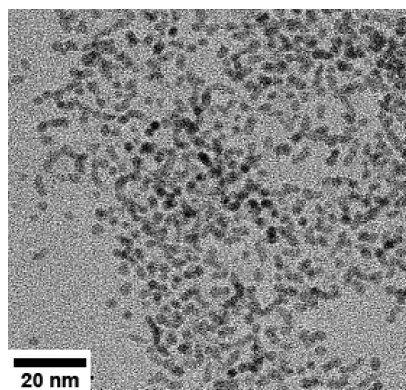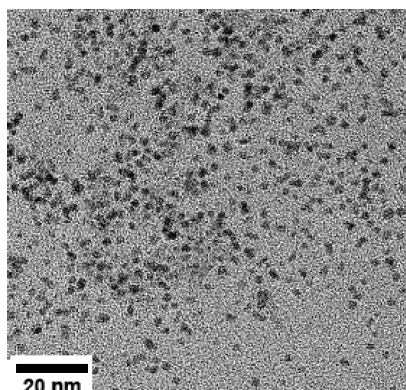
Fig. 6. TEM images of Pt nanoparticles synthesized with a Pt^{4+} concentration of 0.9 mM and PVP concentrations of sample 12, 0.16 mM (left) and sample 10, 0.01 mM (right) at 90 °C/60 min in methanol.
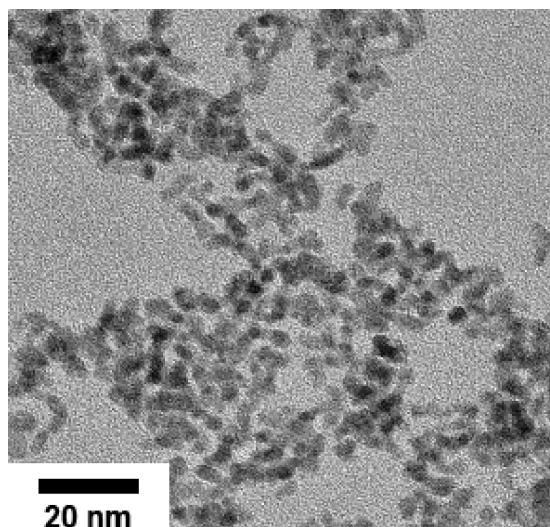

Fig. 7. TEM image of Pt nanorods formed (sample 8) with the PVP concentration of 0.04 mM and the concentration of Pt^{4+} at 0.9 mM at 120 °C with the presence of distilled water.

Fig. 8. TEM Image of Pt nanorods formed (sample 9) with the PVP concentration of 0.04 mM and the concentration of Pt^{4+} at 0.9 mM at 90 °C without the presence of distilled water.

Effect of the PVP concentration on the morphology of Pt nanoparticles

Fig. 6 gives the TEM images of Pt nanoparticles synthesized with different PVP concentrations at 90 °C/60 min. At higher concentrations of PVP (0.16 mM), smaller amounts of nanorods formed as shown in Fig. 6 (left). On the other hand, lower concentrations (0.01 mM) of PVP led to the formation of agglomerated nanorods as shown in Fig. 6 (right). As discussed before, this is probably because at low concentration of PVP, the Pt nanoparticles growing during the reaction would not be fully covered by PVP molecules, which may have led to the preferential growth of nanorods.
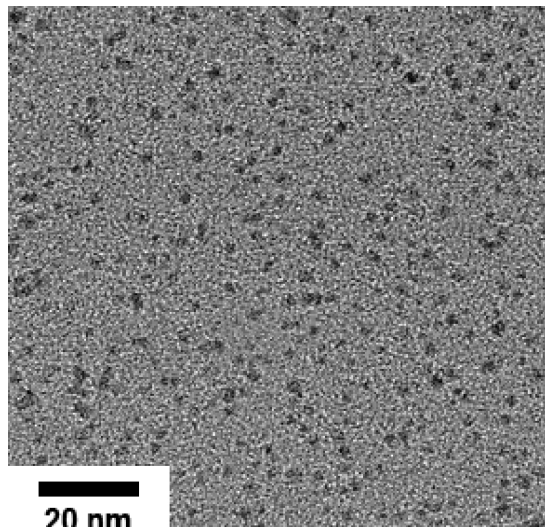
Effects of temperature and distilled water on the morphology of Pt nanoparticles

The temperature and the presence of distilled water affect the morphology of Pt nanoparticles. High temperature (120 °C) and the presence of distilled water favor the formation of agglomerated Pt nanorods. Agglomerated Pt nanorods formed at 120 °C in the presence of distilled water. The reaction rate was increased by the higher temperature of 120 °C. Therefore, more nanorods formed. Fig. 7 shows the TEM image of agglomerated Pt nanorods formed at a concentration of Pt^{4+} of 0.9 mM and a PVP concentration of 0.04 mM at 120 °C. At low temperature (90 °C), the obtained Pt nanoparticles contained both nanorods
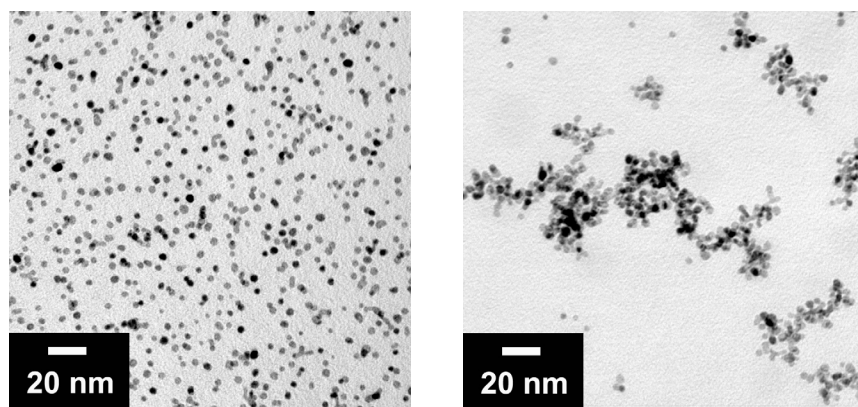
Fig. 9. TEM images of Pt nanoparticles synthesized by the conventional method in an oven at 120 °C for 2 h (left, sample 18) and 4 h (right, sample 19).

Table 3. List of the reaction conditions of the concentrations of chemicals, volumes of methanol, molar ratio of PVP repeating unit to Pt^{4+}, reaction time at 120 °C, and particle size of Pt nanoparticles synthesized by conventional methods.

Sample code	$c_{\text{Metal precursor}}$, (mM) H_2PtCl_6	c_{PVP}, mM MW 40 K	R	V_{methanol}, mL	Time h	Particle size, nm
18	9	0.04	1.8	10	2	3.9 ± 0.6
19	9	0.04	1.8	10	4	–

The particle size of sample 34 is not given due to particle agglomeration.

and nanospheres (shown in Fig. 5 b). Without distilled water, well-dispersed Pt nanospheres were obtained at 90 °C (Fig. 8). The reason why distilled water in the reaction system favored the formation of nanorods is not understood yet.

Comparison of microwave-assisted techniques with conventional methods

Platinum nanoparticles were also synthesized by conventional methods in an oven at 120 °C within 2 and 4 h. Table 3 lists the concentrations of chemicals, volumes of methanol, molar ratio of the PVP repeating units to Pt^{4+}, reaction time and temperature (120 °C). The size of the synthesized Pt nanoparticles after 2 h was 3.9 ± 0.1 nm. The TEM image is shown in Fig. 9 (left). With the reaction time of 4 h, the obtained Pt nanoparticles agglomerated (Fig. 9 (right)). Compared with Pt nanoparticles synthesized by the microwave-assisted method (sample 6 shown in Fig. 1 (left), which were synthesized under the same reaction conditions),

the Pt nanoparticles produced (sample 18) by the conventional method within 2 h have similar morphology. This result is consistent with those obtained for Ag and Pd nanoparticles because these metal ions are easily reduced. The average particle size (3.9 nm) of Pt nanoparticles (sample 18) obtained in an oven within 2 h is slightly larger than that (2.8 nm) of Pt nanoparticles (sample 6) produced by microwave heating for 1 h.

Conclusion

Well-dispersed Pt nanoparticles were obtained using methanol as a reducing agent. The morphology of the Pt nanoparticles is dependent on the temperature, the concentrations of PVP and Pt^{4+}, and the presence or absence of distilled water. Without distilled water in the reaction system, Pt nanospheres were obtained. The particle size was approximately 2 to 3 nm at 120 °C for 60 min. With distilled water in the system, Pt nanorods could be obtained. A higher temperature, a lower concentration of PVP, and a proper concentration of Pt^{4+} favored the formation of Pt nanorods. In addition, Pt nanoparticles were also synthesized using ethanol as a reducing agent at 120 °C. However, the Pt nanoparticles obtained were not dispersed. At 90 °C for 1 h, Pt nanoparticles did not form.

Both microwave-assisted and conventional methods produced Pt nanoparticles with similar morphology and particle size. However, it takes more time to produce particles with similar size by the conventional method with its slower kinetics compared to the microwave-assisted solvothermal method.

[1] A. Roucoux, J. Schulz, H. Patin, Chem. Rev. **102**, 3757 (2002).

[2] Z. Liu, X. Y. Ling, X. Su, J. Y. Lee, J. Phys. Chem. B **108**, 8234 (2004).

[3] Y. Shen, J. Liu, A. Wu, J. Jiang, L. Bi, B. Liu, Z. Li, S. Dong, Langmuir **19**, 5397 (2003).

[4] T. S. Ahmadi, Z. L. Wang, T. C. Green, A. Henglein, M. A. ElSayed, Science **272**, 1924 (1996).

[5] S. Komarneni, D. Li, B. Newalkar, H. Katsuki, A. S. Bhalla, Langmuir **18**, 5959 (2002).

[6] F. Bonet, V. Delmas, S. Grugeon, R. Herrera Urbina, P.-Y. Silvert, K. Tekaia-Elhsissen, Nanostr. Mater. **11**, 1277 (1999).

[7] F. Cea, R. W. Devenish, T. Goulding, B. T. Heaton, C. J. Kiely, A. K. Smith, J. Temple, M. Vargaftik, R. Whyman (ed.), Preparation and Characterization of Platinum-Group Metal Nanoparticles, Vol. 1993, pp. 477–480 (1993).

[8] W.-X. Chen, J. Y. Lee, Z. Liu, Mater. Lett. **58**, 3166 (2004).

[9] K.-S. Kim, D. Demberelnyamba, H. Lee, Langmuir **20**, 556 (2004).

[10] Y.-H. Luo, Z.-L. Jiang, F.-Z. Liu, Guijinshu/Precious Metals **24**, 19 (2003).

[11] Y. Mizukoshi, E. Takagi, H. Okuno, R. Oshima, Y. Maeda, Y. Nagata, Ultras. Sonochem. **8**, 1 (2001).

[12] H.-L. Tang, M. Pan, S.-C. Mu, R.-Z. Yuan, J. Wuhan Univ. Techn., Mater. Sci. Ed. **19**, 7 (2004).

[13] J. Yang, J. Y. Lee, T. C. Deivaraj, H.-P. Too, J. Colloid Interf. Sci. **277**, 95 (2004).

[14] M. Zhao, R. M. Crooks, Adv. Mater. **11**, 217 (1999).

[15] Y. Zhou, H. Itoh, T. Uemura, K. Naka, Y. Chujo, Langmuir **18**, 277 (2002).

[16] R. M. Crooks, M. Q. Zhao, L. Sun, V. Chechik, L. K. Yeung, Acc. Chem. Res. **34**, 181 (2001).

[17] Y. H. Niu, R. M. Crooks, C. R. Chim. **6**, 1049 (2003).

[18] S. Komarneni, H. Katsuki, D. Li, A. S. Bhalla, J. Phys.: Condens. Matter **16**, S1305 (2004).